Journal of Biomechanics 96 (2019) 109344

Contents lists available at ScienceDirect

Journal of Biomechanics

journal homepage: www.elsevier.com/locate/jbiomech
www.JBiomech.com

A comparison of methods to quantify control of the spine

Eric Bourdon [a], Ryan B. Graham [a], Jaap van Dieën [b,*]

[a] School of Human Kinetics, Faculty of Health Sciences, University of Ottawa, 200 Lees Avenue, Ottawa, Ontario K1N 6N5, Canada
[b] Department of Human Movement Sciences, Vrije Universiteit Amsterdam, Amsterdam Movement Sciences, Van der Boechorststraat 9, 1081 BT Amsterdam, Netherlands

ARTICLE INFO

Article history:
Accepted 13 September 2019

Keywords:
Biomechanics
Local dynamic stability
Movement
Systems identification
Lyapunov exponents

ABSTRACT

Low back pain (LBP) affects many individuals worldwide. The established association between LBP and spine motor control has led to the development of many control assessment techniques. To understand spine control and LBP, it is essential to know the relationship between assessment techniques. Systems identification (SI) and local dynamic stability (LDS) are two methods of quantifying spine control. SI provides a detailed description of control but uses linearity assumptions, whereas LDS provides a "black box" non-linear assessment during dynamic movements. Therefore, the purpose of this project was to compare control outcomes of SI and LDS. 15 participants completed two tasks (SI and LDS) in a random order. For the SI task, participants were seated and ventrally perturbed at the 10th thoracic vertebrae. They were instructed to resist the perturbations (resist condition) or to relax the trunk (relax condition). Admittance was computed, and a neuromuscular control model quantified lumbar stiffness, damping and muscle spindle feedback gains. For the LDS task, participants completed three repetitive movement blocks consisting of flexion/extension, axial rotation, and complex movements. In each block, the maximum finite-time Lyapunov exponent (λ_{max}) was estimated. A stepwise linear regression determined that λ_{max} during the rotation task was best predicted by SI outcomes in the relax condition (adjusted $R^2 = 0.83$). Many conditions demonstrated no relationship between λ_{max} and SI outcomes. These findings outline the importance of a consistent framework for the assessment of spine control. This could clarify research comparisons and the understanding of the cause/effect role of LBP on spine control.

1. Introduction

Low back pain (LBP) is still highly prevalent in today's society with a reported 70–85% of individuals experiencing LBP in their lifetime (Andersson, 1999). Despite the magnitude of this issue, the causes of LBP are poorly understood, as in 90% of cases no relation is made to underlying pathology, which are therefore labeled "non-specific" (Krismer and van Tulder, 2007). As understanding the problem is essential to finding a solution, there has been a considerable amount of research dedicated to identifying risk factors associated with the development, progression and recurrence of LBP.

Currently, the association between LBP and changes in spine motor control is well established (e.g., Descarreaux et al., 2005; Freddolini et al., 2014; Radebold et al., 2001); however the exact relationship is largely misunderstood (van Dieën et al., 2018a). This misunderstanding could be due to subgroups existing within the LBP population, or different methodological approaches to the quantification of spine control. Without understanding the relationship between quantification techniques, exact neuromuscular control differences between healthy and LBP populations can be difficult to detect and consolidate. This can lead to misinterpretation of the cause/effect role of spine motor control on LBP.

Local dynamic stability (LDS) is one specific technique for assessing spine motor control, which utilizes kinematic or EMG data obtained during cyclic trunk movements to quantify the spine's response to internal perturbations that occur naturally during movement. LDS quantifies the underlying structure within cyclic biological data through the maximum Lyapunov exponent (λ_{max}), which represents the average exponential rate of divergence of a data point from an attractor/trajectory within a reconstructed state space (Rosenstein et al., 1993). As there is no universally accepted method to design the multidimensional state space (Dingwell, 2006), multiple methods have been proposed within the literature (Gates and Dingwell, 2009). Mainly, the state space has been composed of the Euclidean norm of trunk Euler angles and time-delayed copies (e.g., Beaudette et al., 2014; Granata and Gottipati, 2008), or trunk linear and angular velocities

* Corresponding author at: Department of Human Movement Sciences, VU University Amsterdam, Van der Boechorststraat 9, NL-1081 BT Amsterdam, Netherlands.
E-mail address: j.van.dieen@vu.nl (J. van Diën).

https://doi.org/10.1016/j.jbiomech.2019.109344
0021-9290/

and their time delayed copies (Dupeyron et al., 2013). When using LDS, it is important to consider different state space reconstruction techniques, as they may influence λ_{max} estimations. LDS has been used frequently to identify spine control during repetitive lifting tasks (Graham et al., 2012) and repetitive unloaded trunk movement tasks under different conditions such as LBP (Asgari et al., 2015), movement speed and direction (Granata and England, 2006) and during muscular fatigue (Granata and Gottipati, 2008). LDS has also been used to assess motor control differences in asymmetrical movement tasks (Graham et al., 2014) and during rotational and complex tasks that involved movement in the frontal and transverse planes (Dupeyron et al., 2013). LDS is an advantageous movement control assessment technique as it allows control to be quantified during repetitive dynamic movements that occur frequently in every-day life. While applicability of LDS is good, it only provides a "black box" assessment of spine control. Specifically, although smaller λ_{max} values indicate slower divergence (better performance of trunk control, i.e., faster correction of perturbations) and higher λ_{max} values are indicative of faster divergence (worse control performance), λ_{max} provides no insight into causes of changes in spine control. It is also difficult to identify the λ_{max} cutoffs that identify these phenotypes, as λ_{max} is an arbitrary value that depends on movement type and the system being measured.

Systems identification (SI) is another method that is used to assess neuromuscular control of the spine in an upright posture. To assess control, SI applies known mechanical perturbations to the spine system and measures the response during the disturbances. With these data, the relationship between the input and output of the spine system is represented by frequency response functions (FRFs) that allow for quantification of intrinsic and reflexive contributions to spine control (Goodworth and Peterka, 2009; van Dieën et al., 2018b; van Drunen et al., 2013). Most of these studies have applied perturbations to the trunk in an upright seated posture in the sagittal plane where subjects were instructed to either maximally resist the perturbations or to relax and control posture as felt natural. This approach has been instrumental in identifying the importance of reflex dynamics for postural control (Moorhouse and Granata, 2007) and revealed how control parameters are modulated with instruction and perturbation type (van Dieën et al., 2018b; van Drunen et al., 2015). While the detail provided by SI is useful, application is limited to instances that can be regarded as approximately linear. Therefore, it is unclear whether findings from SI techniques can be generalized to dynamic movements.

Both LDS and SI have been frequently used to assess spine control, however the relationship between the outcomes of these two techniques is unknown. It is possible that control mechanisms, despite different task demands in SI and LDS, are similar between the two tasks as both methods aim to quantify stabilization of a trunk posture (SI) or a trunk movement trajectory (LDS). For instance, intrinsic stiffness of the trunk may be similar between tasks when similar postures are assumed, and reflexive properties such as muscle spindle feedback may contribute to control in both tasks. Therefore, although there may be overlap in the control mechanisms between tasks, the magnitude of overlap is unknown. This provides a barrier to summarizing literature relating to the cause/effect role of LBP on movement control, as findings from SI and LDS may be difficult to directly compare. In addition, as LDS can be quantified during dynamic movement, and SI during upright static posture, the relationship between these outcomes could provide information as to whether static postural control strategies are similar to control strategies recruited during dynamic movements. Therefore, the purpose of this project is to understand the relationship between motor control outputs of LDS and SI to: (i) improve the understanding of direct comparisons, and (ii) identify if linear postural control strategies relate to dynamic control strategies. It was hypothesized that control strategies would be most similar between LDS during flexion/extension movements, because both tasks involve sagittal plane movements. It is also hypothesized that similar control strategies would be utilized between LDS and SI outcomes under relax task instructions, a natural response to perturbations in both the LDS and SI task under relax instructions is expected.

2. Methods

2.1. Participants

Nine male and six female participants were recruited to participate in this study. Participants' mean age, height, mass and the associated standard deviations (SD) were 35.5 years (SD = 12.5), 175.4 cm (SD = 8.5) and 72.9 kg (SD = 11.6), respectively. Participant demographics (separated by sex) are presented in Table 1. All participants acknowledged that they were healthy and had not experienced an episode of LBP within the past year, or a major musculoskeletal injury within the past six months before participation. All procedures were reviewed and approved by ethical review boards at the University of Ottawa (#H02-17-11) and Vrije Universiteit Amsterdam (#VCWE-2017-146). All data were collected at Vrije Universiteit Amsterdam.

2.2. Instrumentation

2.2.1. Local dynamic stability

The three-dimensional positions of the trunk and pelvis were tracked using two active marker clusters adhered over the T_{10}-T_{12} vertebra and the sacrum to determine motion of the lumbar spine. Data were collected at 100 Hz using two Optotrak 3020 motion capture cameras (Optotrak3020, Northern Digital, Inc., Canada). In addition, a digital pointer was used to identify the location of anatomical landmarks on the trunk and pelvis (all landmarks included in supplementary material 1) for calculation of segment coordinate systems.

2.2.2. Systems identification

Surface electromyography (sEMG) data were collected (sEMG REFA, TMSi, the Netherlands) using pairs of bipolar electrodes (Ag/AgCl, inter-electrode distance 25 mm). A custom-built apparatus was used to hold participants in a seated kneeling posture (Fig. 1). Participants were perturbed with a magnetically-driven linear actuator (Servotube STB2510S Forcer and Thrustrod TRB25-1380, Copley Controls, USA). Actuator displacement (representing spine kinematics) and contact force between the actuator and participant were collected at 2000 Hz using an instrumented probe (Servotube position sensor & Force sensor FS6-500, AMTI, USA).

Table 1
Participant demographics.

	Height (cm)	Mass (kg)	Age (years)
	Mean (SD)	Mean (SD)	Mean (SD)
Male	179.2 (7.0)	77.6 (10.0)	34.1 (12.0)
Female	169.6 (7.0)	65.7 (9.9)	37.5 (13.0)
All	175.4 (8.5)	72.9 (11.6)	35.5 (12.5)

All participants were recruited from the general university employee and student population. All participants met the inclusion criteria. SD = standard deviation.

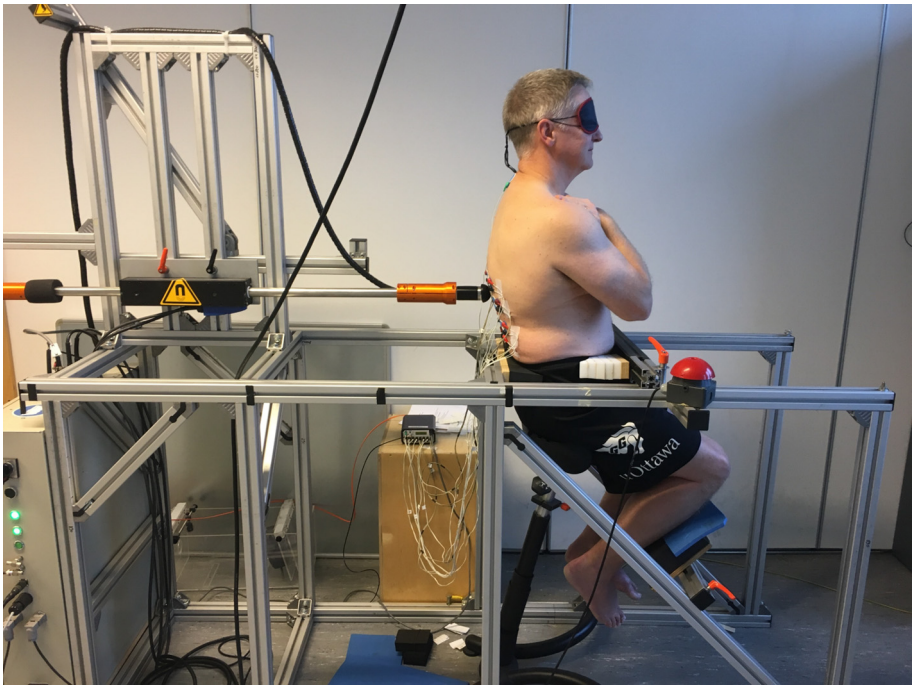

Fig. 1. Participant set-up for completion of Task B (SI).

2.3. Protocol

Following informed consent and collection of demographic data, participants completed task A (LDS) and task B (SI) in a randomized order. Active marker clusters were worn during the LDS task and sEMG sensors were worn during the SI task.

Task A (LDS) involved participants completing three blocks of repetitive trunk movement tasks in a randomized order (Dupeyron et al., 2013). The first block consisted of 35 cycles of repetitive forward flexion and extension (FE block; Fig. 2A). Specifically, participants touched a target at shoulder height and knee height repeatedly with a movement cycle frequency of 15 cycles per minute (4 s/cycle) to a metronome playing at 0.5 Hz; participants were instructed to keep their arms outstretched directly in front of them. This instruction was provided to ensure that most of the movement occurred through the spine. During the other tasks, no specific instructions for arm placement was provided as they were inherently impossible to be completed without large movements of the spine.

For the second block, participants completed 35 cycles of repeated axial rotation (rotation block; Fig. 2B) alternating between touching a target placed on their right side with their left hand and a target placed on their left side with their right hand. Targets were placed at shoulder height and at an arm's length away. Metronome and cycle frequency were identical to the FE block.

The third block (complex block; Fig. 2C) consisted of the participant completing 35 cycles of touching a target located at shoulder height on the right side, shoulder height on the left side, knee height on the right side and finally knee height on the left side consecutively to the beat of a metronome at 0.5 Hz. This resulted in a movement frequency of 8 s/cycle. Although these movement tasks

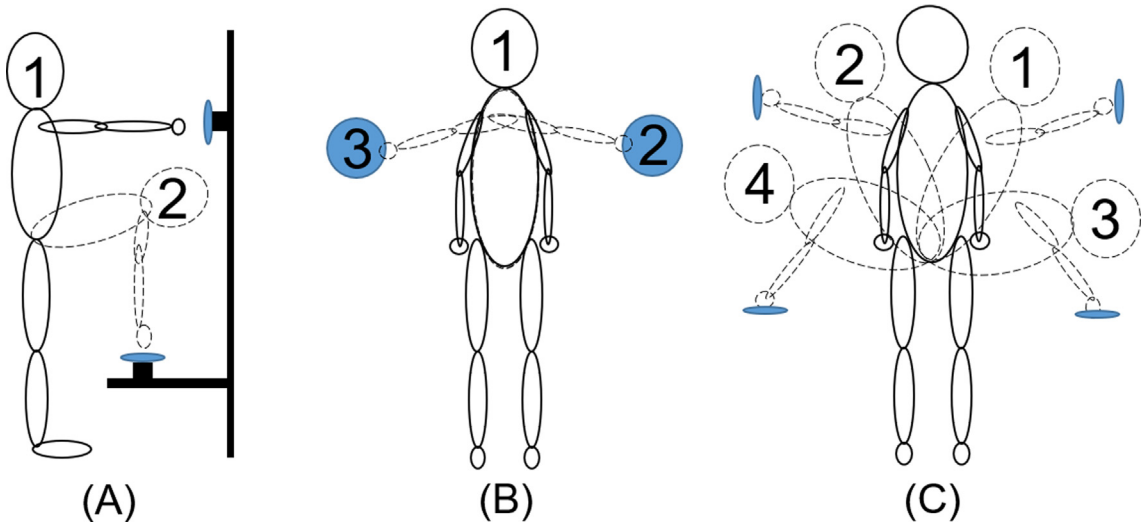

Fig. 2. Series of trunk movements for task A (LDS), (A) flexion/extension block, (B) rotation block, (C) complex block.

required minimal effort, rest periods in between blocks were provided to prevent any effect of fatigue.

Task B (SI) began with skin preparation and placement of sEMG sensors. Pairs of sEMG electrodes were placed on the longissimus (thoracic and lumbar) and iliocostalis (thoracic and lumbar) muscles according to Willigenburg et al. (2010). Following attachment of sEMG sensors, participants were placed in a seated-kneeling posture, and restrained at the pelvis to prevent any movement. Participants were blindfolded and instructed to cross their arms across their chest for the duration of the trial (Fig. 1); a magnetically-driven linear actuator was positioned level with the T_{10} spinous process and in-contact with the spine. In this position, participants were exposed to fifty seconds of dynamic disturbances in which the linear actuator applied pseudorandom force perturbations. The pseudorandom force signal was designed identical to that of van Drunen et al. (2013). Three trials in each instruction condition (resist and relax) were completed (six trials total) in a randomized order. Specifically, the resist instructions were to maximally resist the force perturbations and remain upright for the entire trial. This task instruction was given to measure the individual's maximum level of control. In contrast, the relax instructions were to relax the trunk as much as possible; however, to remain upright following a perturbation. This task instruction was given to quantify a more natural response to mechanical perturbations.

2.4. Data processing and analysis

2.4.1. Local dynamic stability

All kinematic operations were calculated using custom MATLAB software (R2017A, The MathWorks, Inc., USA). All kinematic data were first filtered using a 2nd order lowpass zero-lag Butterworth filter with a 10 Hz cut-off frequency (Moorhouse and Granata, 2005). Right hand local coordinate systems for the trunk and pelvis were calculated based on the locations of anatomical landmarks, and the three-dimensional location of these segments were tracked using their associated marker clusters. Three-dimensional lumbar spine angles were calculated using Euler rotation matrices (flexion-extension/lateral bending/axial twist sequence) of the trunk coordinate system relative to that of the pelvis. Linear velocity of the trunk was defined as the first derivative of the trunk position relative to the pelvis. Trunk angular velocity was defined as the decomposed first derivative of the relative orientation matrix between the trunk and pelvis.

Kinematic data were divided into cycles and the last 30 were selected for analysis to allow the participant to reach a steady-state movement pattern. Each block was normalized to a length determined by Eq. (1), as the number of samples can affect LDS estimates (Bruijn et al., 2009).

$$\#ofsamples = \#ofcycles \times cycletime(s) \times samplefrequency \quad (1)$$

Two popular state space reconstruction techniques were explored (6D and 12D). For the 6D technique, lumbar spine Euler angles were first biased into a positive Cartesian space to remove any zero crossings and relative bias between movement planes (Beaudette et al., 2016). Similar to Graham et al. (2014), a 6-dimensional state-space (Y(t)) was reconstructed using the Euclidean norm of the 3-dimensional lumbar spine angle (r) at each time point (t) and its time-lagged (T_L) versions as per Eq. (2) (6D technique).

$$Y(t) = [r(t), r(t+T_L), r(t+2T_L), \cdots, r(t+5T_L)] \quad (2)$$

For the 12D technique, the state was reconstructed similar to Dupeyron et al. (2013), where a 12-dimensional state-space ($Y(t)$) was reconstructed using the trunk's linear ($\dot{x}$,$\dot{y}$, $\dot{z}$) and angular ($\dot{\theta}$,$\dot{\varphi}$, $\dot{\tilde{N}}\pm$) velocities and their time-lagged (L) copies as per Eq. (3).

$$Y(t) = \begin{bmatrix} \dot{x}_1 & \dot{y}_1 & \dot{z}_1 & \dot{\theta}_1 & \dot{\varphi}_1 & \dot{\psi}_1 & \dot{x}_{L1} & \dot{y}_{L1} & \dot{z}_{L1} & \dot{\theta}_{L1} & \dot{\varphi}_{L1} & \dot{\psi}_{L1} \\ \dot{x}_2 & \dot{y}_2 & \dot{z}_2 & \dot{\theta}_2 & \dot{\varphi}_2 & \dot{\psi}_2 & \dot{x}_{L2} & \dot{y}_{L2} & \dot{z}_{L2} & \dot{\theta}_{L2} & \dot{\varphi}_{L2} & \dot{\psi}_{L2} \\ \cdots & \cdots & \cdots & \cdots & \cdots & \cdots & \cdots & \cdots & \cdots & \cdots & \cdots & \cdots \\ \dot{x}_n & \dot{y}_n & \dot{z}_n & \dot{\theta}_n & \dot{\varphi}_n & \dot{\psi}_3 & \dot{x}_{Ln} & \dot{y}_{Ln} & \dot{z}_{Ln} & \dot{\theta}_{Ln} & \dot{\varphi}_{Ln} & \dot{\psi}_{L3} \end{bmatrix} \quad (3)$$

In both methods of state-space reconstruction, a time-lag of 10% of the cycle length (40 frames for flexion/extension and rotation block, 80 frames for complex block) was selected (Bruijn et al., 2009; England and Granata, 2007; Granata and England, 2006; Howarth et al., 2013). Within both state-spaces, nearest neighbor trajectories and the exponential rate of divergence between these were identified (Rosenstein et al., 1993). The average rate of divergence between all nearest neighbor pairs was plotted over a period from 0 to 1 cycle, and λ_{max} was estimated as the slope of a line of best fit spanning 0–0.5 cycles (Graham et al., 2012). λ_{max} was calculated for all repetitive movement blocks and state space reconstruction techniques.

2.4.2. Systems identification

sEMG data were zero phase, first order, high-pass filtered at 250 Hz before being rectified (Staudenmann et al., 2007).

Actuator displacement, contact force and sEMG data were collected and synchronized using customized software and analyzed in MATLAB (R2017A, The MathWorks Inc., USA). Closed-loop identification techniques (Schouten et al., 2008) were used to represent the admittance ($H_{adm}(f)$; Eq. (4)) and reflexes ($H_{emg}(f)$; Eq. (5)) as FRFs. The admittance FRF describes the actuator displacement ($X_A(t)$) as a function of the contact force ($F_c(t)$), while reflex FRFs describe the sEMG ($e(t)$) data as a function of the actuator displacement.

$$H_{adm}(f) = \frac{S_{F_pX_A}(f)}{S_{F_pF_c}(f)} \quad (4)$$

$$H_{emg}(f) = \frac{S_{F_pe}(f)}{S_{F_pX_A}(f)} \quad (5)$$

where $S_{F_pX_A}(f)$, $S_{F_pF_c}(f)$ and $S_{F_pe}(f)$ represent the estimated cross-spectral densities between the Fourier transformed force-perturbation ($F_p(f)$) and actuator displacement ($X_A(f)$), contact force ($F_c(f)$) and sEMG ($e(f)$), respectively (Maaswinkel et al., 2015). Cross-spectral densities were only calculated at the frequencies in which the participants were perturbed. Densities were averaged across six time segments (three trials with two 20 s dynamic disturbances) and over two adjacent frequency points. Lastly, $S_{F_pe}(f)$ was averaged over the left and right muscles.

Coherence represents the relationship between the input and the output of the system. Coherence of admittance ($H_{adm}(f)$) and reflexes ($H_{emg}(f)$)were derived using Eqs. (6) and (7), respectively (van Drunen et al., 2013). Due to spectral densities being averaged over 12 points, coherence of over 0.24 was considered significant at $p < 0.05$ (Halliday et al., 1996). Only coherence at the frequencies that reached this significance level were used for analysis. A coherence of 1 would represent a perfect relation between the input and output whereas a coherence of 0 would represent no relation between the two.

$$\gamma^2_{adm}(f) = \frac{|S_{F_pX_a}(f)|^2}{S_{F_pF_p}(f)S_{X_AX_A}(f)} \quad (6)$$

$$\gamma^2_{emg}(f) = \frac{|S_{F_pe}(f)|^2}{S_{F_pF_p}(f)S_{ee}(f)} \quad (7)$$

FRFs were averaged across trials within each condition (relax, resist) to improve precision of outcomes and subsequently used in a previously described neuromuscular control model to quantify additional intrinsic and reflexive properties of the spine (van Dieën et al., 2018b). Specifically, the model quantified lumbar intrinsic stiffness (K) and damping (B), which consider the viscoelastic properties of muscles and passive tissues, as well as feedback gain from muscle spindle position (K_p), velocity (K_v) and acceleration (K_a). These parameters were calculated in both the resist and relax conditions.

2.4.3. Statistical analysis

All statistical calculations were performed in SPSS (v23, IBM Corporation, USA). A forward selection step-wise linear regression was used to define regression models with λ_{max} from each movement block as the dependent variable (DV) and outputs of SI from each task as the independent variables (IV). Specifically, the IVs assigned were the: admittance gain at 0.22, 0.33, 0.48, 0.73 and 1.08 Hz, muscle spindle (MS) position (K_p), velocity (K_v) and acceleration (K_a) feedback gains as well as lumbar intrinsic stiffness (K) and damping (B; Table 2), as these are thought to be closely related to movement control (van Dieën et al., 2018b). The probability for an IV to enter the model was $p < 0.2$, and the probability to exit the model was $p > 0.3$. Models were considered valid if the F-test significance was less than the alpha of 0.05 ($p < 0.05$). The adjusted R-square value for each model was calculated using the default SPSS adjustment, and is presented as a percentage of the variance in λ_{max} that is described by the IVs included in the model. λ_{max} in each task and state-space reconstruction technique was compared to SI outputs in the relax and resist tasks separately. Variance inflation factor (VIF) was used as an indicator of collinearity and is presented for each model.

3. Results

3.1. 6D state space reconstruction

Results presented in this section are linear regression models associated with λ_{max} estimations using the 6-dimensional state space technique. The strongest predictive models for all comparisons are summarized below and included in Table 3. All predictive models have been included in supplementary material 2.

3.1.1. FE block

Admittance gain at 1.08 Hz ($\beta = 355.1$, $p = 0.05$) in the relax task predicted 20.7% ($R^2_{adj} = 0.207$, $p = 0.05$) of the variance in λ_{max} during the FE block.

Admittance gain at 0.73 Hz ($\beta = 995.8$, $p = 0.025$), K_a ($\beta = 0.002$, $p = 0.039$) and K_v ($\beta = -0.0001$, $p = 0.088$) in the resist task predicted 37.7% ($R^2_{adj} = 0.377$, $p = 0.042$) of the variance in λ_{max} during the FE block.

3.1.2. Rotation block

Admittance gain at 0.23 ($\beta = 433.5$, $p = 0.003$) and 0.33 Hz ($\beta = -1682.7$, $p = 0.001$), K_p ($\beta = 0.00007$, $p = 0.001$), K_v ($\beta = -0.0003$, $p < 0.001$), K ($\beta = -0.00007$, $p = 0.005$) and B ($\beta = 0.0001$, $p = 0.03$) in the relax task predicted 83.1% ($R^2_{adj} = 0.831$, $p = 0.001$) of the variance in λ_{max}.

No SI variables in the resist task significantly predicted λ_{max} in the rotation block.

3.1.3. Complex block

No SI variables in the relax or resist task significantly predicted λ_{max} values calculated during the complex movement block.

3.2. 12D state space reconstruction

All results presented in this section are linear regression models associated with λ_{max} estimations using a 12-dimensional state space reconstructed using the linear and angular velocities of the trunk relative to the pelvis and their time-delayed versions. The strongest predictive models in each comparison are summarized in Table 4. All predictive models have been included in supplementary material 2.

3.2.1. FE block

No regression models in the relax or resist task reached the critical significance level ($p < 0.05$) to predict λ_{max} calculations during the FE block.

3.2.2. Rotation block

No regression models in the relax or resist task reached the critical significance level ($p < 0.05$) to predict λ_{max} calculations during the Rotation block.

3.2.3. Complex block

In the relax task, the model including admittance gain at 0.73 Hz ($\beta = -858.6$, $p = 0.007$) as well as lumbar damping ($\beta = -0.0005$, $p = 0.008$) predicted 43.1% ($R^2_{adj} = 0.431$, $p = 0.013$) of the variance in λ_{max}.

No regression models in the resist task reached the critical significance level ($p < 0.05$) to predict λ_{max} calculations during the Rotation block.

4. Discussion

The purpose of this study was to compare the outcomes of two spine control quantification techniques, namely, LDS and SI. Overall, SI variables were only able to strongly explain variance in λ_{max} under very specific conditions. Overall, it is clear that results from linear postural control assessment may not be directly compared to dynamic control strategies as potential mechanical and feedback differences lead to altered control recruitment strategies. This outlines the importance of understanding control assessment techniques and the demand for a consistent framework for comprehensive spine control assessment to confidently identify the role of spine motor control in LBP.

As hypothesized, SI control outcomes in the relax condition demonstrated the strongest relationship with λ_{max} values, describing up to 83.1% of the variance in λ_{max}. In contrast, SI outcomes during resist task instructions significantly explained variance in λ_{max} only on one occasion, describing 37.7% of the variance in λ_{max}. The difference in findings between relax and resist tasks may be attributable to the nature of each task and the task instructions. The SI relax condition is designed to quantify a natural response to external perturbations, whereas the resist task is meant to

Table 2
Format for set-up of stepwise linear regression.

DV	IV Admittance gain (Hz)									
λ_{max}	0.23	0.33	0.48	0.73	1.08	K	B	K_p	K_v	K_a

Table 3
Strongest predictive models when using the 6D technique for λ_{max} estimation.

		SI Relax			Resist		
		%	*p*	VIF	%	*p*	VIF
λ_{max}	Flexion/extension	20.7[a]	**0.05**	1.00	37.7[b]	**0.042**	11.91
	Rotation	83.1[c]	**<0.001**	7.71	No significant model		
	Complex	No significant model			No significant model		

[a] Predictors: admittance gain at 1.08 Hz.
[b] Predictors: admittance gain at 0.73 Hz, K_a and K_v.
[c] Predictors: admittance gain at 0.23 Hz, K_p and K_v.

Table 4
Strongest predictive models when using the 12D technique for λ_{max} estimation.

		SI Relax			Resist		
		%	*p*	VIF	%	*p*	VIF
λ_{max}	Flexion/extension	14.0[a]	0.095	1.00	15.8[b]	0.079	1.00
	Rotation	23.8[c]	0.117	2.50	9.7[d]	0.138	1.00
	Complex	43.1[e]	**0.013**	1.72	6.2[d]	0.189	1.00

[a] Predictors: admittance gain at 1.08 Hz.
[b] Predictors: admittance gain at 0.48 Hz.
[c] Predictors: admittance gain at 0.73 and 1.08 Hz.
[d] Predictors: B.
[e] Predictors: admittance gain at 0.73 Hz and B.

quantify an individual's maximum resistance to perturbations. Although participants were slightly constrained by the metronome frequency in the LDS task, there were no instructions given to maximize movement control. Given that LDS is not purely a tracking task, but a means to quantify the short-term response to internal perturbations, a fairly natural movement pattern is likely demonstrated. Therefore, both SI during relax instructions and LDS could be quantifying a natural response to kinematic disturbances.

Contrary to the hypothesis, LDS in the FE block did not demonstrate the strongest relationship with SI outcomes. This may have been due to the large range of motion in the FE block, as it is understood that different control strategies are utilized in flexed postures (Maaswinkel et al., 2015). In fact, despite movement in the transverse plane, the rotation block demonstrated the strongest relationship with SI outcomes. A potential explanation for this relationship is the shared postural demands between tasks. Specifically, both tasks require an upright trunk posture for the entire duration. This may have caused similar feedback properties and subsequently, similar control strategies to be recruited.

In addition to consideration of the positive results, it is also important to interpret the lack of variance that can be explained when comparing some outputs of SI and LDS. Apparently, in most conditions, movement control strategies are different, and these quantification techniques capture different behavior. When considering that motor behavior is influenced by noise (in both the afferent, sensory and efferent information), task context and the nature of the sensory feedback itself (Scott, 2004), it is likely that one or all of these influencers are different between LDS and SI tasks. This would result in recruitment of different motor control strategies, and subsequent differences in outcomes of motor control assessment techniques. Therefore, confusion may arise when summarizing literature that uses LDS and SI to quantify motor control changes, making the exact effect of conditions like LBP on spine motor control difficult to identify.

These results demonstrate that outcome measures of LDS and SI should be compared with caution as they are only moderately associated and only in specific conditions. As spine control and how it is achieved in different populations (i.e., LBP) is poorly understood, knowing this interaction between outcome measures of LDS and SI is a key component in clarifying the overall understanding of spine control. This supports the need for clear and consistent methodology to assessing spine control. Even within LDS, there are differences in the statistical models between 6D and 12D state space reconstruction techniques, despite the expectation that the results would demonstrate similar trends (Gates and Dingwell, 2009). This difference could be attributed to differences in signal noise and subsequent instability in divergence curves; however, this should be considered when selecting a reconstruction technique.

Within LDS and SI, there are some limitations that exist. Mainly, current SI techniques assume linear behavior, although non-linearities can be captured by parameter variation between conditions and specifically between conditions with different perturbation magnitudes. This implies that perturbations must be constrained to avoid strong non-linearities on the behavior and that the resulting non-parametric and parametric models describe linearised system behavior under the tested, by necessity constrained, condition only. This reflects the difficulty in quantifying the response of the complex spine system. LDS attempts to represent the response of the entire complex spine system using λ_{max}. This provides no detail into the mechanisms of control and creates difficulties when summarizing outcomes between studies with multiple outcome measures (such as SI). Additionally, both LDS and SI should both be refined individually as movement control assessment techniques to improve reliability of measurements and this should be the focus of future research efforts. It is clear that a consistent methodological approach to quantifying spine control would improve the understanding of spine motor control.

Declaration of Competing Interest

The authors declared that there is no conflict of interest.

Acknowledgements

This study was funded by the Natural Sciences and Engineering Research Council of Canada (RGPIN-2014-05560 [Ryan Graham]).

Appendix A. Supplementary material

Supplementary data to this article can be found online at https://doi.org/10.1016/j.jbiomech.2019.109344.

References

Andersson, G.B., 1999. Epidemiological features of chronic low-back pain. Lancet 354, 581–585. https://doi.org/10.1016/S0140-6736(99)01312-4.

Asgari, M., Sanjari, M.A., Mokhtarinia, H.R., Moeini Sedeh, S., Khalaf, K., Parnianpour, M., 2015. The effects of movement speed on kinematic variability and dynamic stability of the trunk in healthy individuals and low back pain patients. Clin. Biomech. 30, 682–688. https://doi.org/10.1016/j.clinbiomech.2015.05.005.

Beaudette, S.M., Graham, R.B., Brown, S.H.M., 2014. The effect of unstable loading versus unstable support conditions on spine rotational stiffness and spine stability during repetitive lifting. J. Biomech. 47, 491–496. https://doi.org/10.1016/j.jbiomech.2013.10.055.

Beaudette, S.M., Howarth, S.J., Graham, R.B., Brown, S.H.M., 2016. On the use of a Euclidean norm function for the estimation of local dynamic stability from 3D kinematics using time-delayed Lyapunov analyses. Med. Eng. Phys. 38, 1139–1145. https://doi.org/10.1016/j.medengphy.2016.07.001.

Bruijn, S.M., van Dieën, J.H., Meijer, O.G., Beek, P.J., 2009. Statistical precision and sensitivity of measures of dynamic gait stability. J. Neurosci. Methods 178, 327–333. https://doi.org/10.1016/j.jneumeth.2008.12.015.

Descarreaux, M., Blouin, J.S., Teasdale, N., 2005. Repositioning accuracy and movement parameters in low back pain subjects and healthy control subjects. Eur. Spine J. 14, 185–191. https://doi.org/10.1007/s00586-004-0833-y.

Dingwell, J.B., 2006. Lyapunov exponents. Wiley Encycl. Biomed. Eng. 20. https://doi.org/10.1002/9780471740360.ebs0702.

Dupeyron, A., Rispens, S.M., Demattei, C., van Dieën, J.H., 2013. Precision of estimates of local stability of repetitive trunk movements. Eur. Spine J. 22, 2678–2685. https://doi.org/10.1007/s00586-013-2797-2.

England, S.A., Granata, K.P., 2007. The influence of gait speed on local dynamic stability of walking. Gait Posture 25, 172–178. https://doi.org/10.1016/j.gaitpost.2006.03.003.

Freddolini, M., Strike, S., Lee, R.Y.W., 2014. Stiffness properties of the trunk in people with low back pain. Hum. Mov. Sci. 36, 70–79. https://doi.org/10.1016/j.humov.2014.04.010.

Gates, D.H., Dingwell, J.B., 2009. Comparison of different state space definitions for local dynamic stability analyses. J. Biomech. 42, 1345–1349. https://doi.org/10.1016/j.jbiomech.2009.03.015.

Goodworth, A.D., Peterka, R.J., 2009. Contribution of sensorimotor integration to spinal stabilization in humans. J. Neurophysiol. 496–512. https://doi.org/10.1152/jn.00118.2009.

Graham, R.B., Oikawa, L.Y., Ross, G.B., 2014. Comparing the local dynamic stability of trunk movements between varsity athletes with and without non-specific low back pain. J. Biomech. 47, 1459–1464. https://doi.org/10.1016/j.jbiomech.2014.01.033.

Graham, R.B., Sadler, E.M., Stevenson, J.M., 2012. Local dynamic stability of trunk movements during the repetitive lifting of loads. Hum. Mov. Sci. 31, 592–603. https://doi.org/10.1016/j.humov.2011.06.009.

Granata, K.P., England, S.A., 2006. Stability of dynamic trunk movement. Spine (Phila. Pa. 1976) 31, E271–E276. https://doi.org/10.1097/01.brs.0000216445.28943.d1.

Granata, K.P., Gottipati, P., 2008. Fatigue influences the dynamic stability of the torso. Ergonomics 51, 1258–1271. https://doi.org/10.1080/00140130802030722.

Halliday, D.M., Rosenberg, J.R., Amjad, A.M., Breeze, P., Conway, B.A., Farmer, S.F., 1996. A framework for the analysis of mixed time series/point process data – theory and application to the study of physiological tremors, single motor unit discharges and electromyograms. Prog. Biophys. Mol. Biol. 64, 237–278.

Howarth, S.J., Kingston, D.C., Brown, S.H.M., Graham, R.B., 2013. Viscoelastic creep induced by repetitive spine flexion and its relationship to dynamic spine stability. J. Electromyogr. Kinesiol. 23, 794–800. https://doi.org/10.1016/j.jelekin.2013.04.002.

Krismer, M., van Tulder, M., 2007. Low back pain (non-specific). Best Pract. Res. Clin. Rheumatol. 21, 77–91. https://doi.org/10.1016/j.berh.2006.08.004.

Maaswinkel, E., van Drunen, P., Veeger, D.J.H.E.J., van Dieën, J.H., 2015. Effects of vision and lumbar posture on trunk neuromuscular control. J. Biomech. 48, 298–303. https://doi.org/10.1016/j.jbiomech.2014.11.030.

Moorhouse, K.M., Granata, K.P., 2007. Role of reflex dynamics in spinal stability: intrinsic muscle stiffness alone is insufficient for stability. J. Biomech. 40, 1058–1065. https://doi.org/10.1016/j.jbiomech.2006.04.018.

Moorhouse, K.M., Granata, K.P., 2005. Trunk stiffness and dynamics during active extension exertions. J. Biomech. 38, 2000–2007. https://doi.org/10.1016/j.jbiomech.2004.09.014.

Radebold, A., Cholewicki, J., Polzhofer, G.K., Greene, H.S., 2001. Impaired postural control of the lumbar spine is associated with delayed muscle response times in patients with chronic idiopathic low back pain. Spine (Phila. Pa. 1976) 26, 724–730. https://doi.org/10.1097/00007632-200104010-00004.

Rosenstein, M.T., Collins, J.J., De Luca, C.J., 1993. A practical method for calculating largest Lyapunov exponents from small data sets. Phys. D Nonlin. Phenom. 65, 117–134. https://doi.org/10.1016/0167-2789(93)90009-P.

A.C. Schouten E. De Vlugt J.J. Van Hilten F.C. Van Der Helm 2008. Quantifying proprioceptive reflexes during position control of the human arm. Hand 55, 311–321.

Scott, S.H., 2004. Optimal feedback control and the neural basis of volitional motor control. Nat. Rev. Neurosci. 5, 532–546. https://doi.org/10.1038/nrn1427.

Staudenmann, D., Potvin, J.R., Kingma, I., Stegeman, D.F., van Dieën, J.H., 2007. Effects of EMG processing on biomechanical models of muscle joint systems: sensitivity of trunk muscle moments, spinal forces, and stability. J. Biomech. 40, 900–909. https://doi.org/10.1016/j.jbiomech.2006.03.021.

van Dieën, J.H., Reeves, N.P., Kawchuk, G., van Dillen, L., Hodges, P.W., 2018a. Motor control changes in low-back pain: divergence in presentations and mechanisms. J. Orthop. Sport. Phys. Ther. 1–24. https://doi.org/10.2519/jospt.2019.7917.

van Dieën, J.H., van Drunen, P., Happee, R., 2018b. Sensory contributions to stabilization of trunk posture in the sagittal plane. J. Biomech. 70, 219–227. https://doi.org/10.1016/j.jbiomech.2017.07.016.

van Drunen, P., Koumans, Y., van der Helm, F.C.T., van Dieën, J.H., Happee, R., 2015. Modulation of intrinsic and reflexive contributions to low – back stabilization due to vision, task instruction, and perturbation bandwidth. Exp. Brain Res. 233, 735–749. https://doi.org/10.1007/s00221-014-4151-2.

van Drunen, P., Maaswinkel, E., van der Helm, F.C.T., van Dieën, J.H., Happee, R., 2013. Identifying intrinsic and reflexive contributions to low-back stabilization. J. Biomech. 46, 1440–1446. https://doi.org/10.1016/j.jbiomech.2013.03.007.

Willigenburg, N.W., Kingma, I., Van Dieën, J.H., 2010. How is precision regulated in maintaining trunk posture? Exp. Brain Res. 203, 39–49. https://doi.org/10.1007/s00221-010-2207-5.